Gen Relativ Gravit (2011) 43:3099–3126
DOI 10.1007/s10714-011-1226-2

RESEARCH ARTICLE

Constraining spacetime torsion with LAGEOS

Riccardo March · Giovanni Bellettini · Roberto Tauraso · Simone Dell'Agnello

Received: 15 December 2010 / Accepted: 10 July 2011 / Published online: 24 July 2011

Abstract We compute the corrections to the orbital Lense-Thirring effect (or frame-dragging) in the presence of spacetime torsion. We analyze the motion of a test body in the gravitational field of a rotating axisymmetric massive body, using the parametrized framework of Mao, Tegmark, Guth and Cabi. In the cases of autoparallel and extremal trajectories, we derive the specific approximate expression of the corresponding system of ordinary differential equations, which are then solved with methods of Celestial Mechanics. We calculate the secular variations of the longitudes of the node and of the pericenter. We also show how the LAser GEOdynamics Satellites (LAGEOS) can be used to constrain torsion parameters. We report the experimental constraints obtained using both the nodes and perigee measurements of the orbital Lense-Thirring effect. This makes LAGEOS and Gravity Probe B complementary frame-dragging and torsion experiments, since they constrain three different combinations of torsion parameters.

R. March (✉)
Istituto per le Applicazioni del Calcolo, CNR, Via dei Taurini 19, 00185 Rome, Italy
e-mail: r.march@iac.cnr.it

R. March · G. Bellettini · R. Tauraso · S. Dell'Agnello
INFN-Laboratori Nazionali di Frascati (LNF), via E. Fermi 40, Frascati, 00044 Rome, Italy

S. Dell'Agnello
e-mail: Simone.Dellagnello@lnf.infn.it

G. Bellettini · R. Tauraso
Dipartimento di Matematica, Università di Roma "Tor Vergata",
via della Ricerca Scientifica 1, 00133 Rome, Italy
e-mail: Giovanni.Bellettini@lnf.infn.it

R. Tauraso
e-mail: tauraso@mat.uniroma2.it

Keywords Riemann-Cartan spacetime · Torsion · Autoparallel trajectories · Frame dragging · Geodetic precession · Satellite laser ranging · Gravity Probe B

1 Introduction

In recent years a lot of effort has been devoted to measure gravitomagnetic effects due to Earth's rotation [1–3] predicted by the theory of General Relativity (GR). In particular, the Lense-Thirring effect on the orbital motion of a test body can be measured by using the satellite laser ranging (SLR) technique, whose data are provided by the ILRS[1]. By analyzing the laser ranging data of the orbits of the satellites LAGEOS and LAGEOS II, a measurement of the Lense-Thirring effect was obtained by Ciufolini and Pavlis [4].

SLR missions can also be useful to test modifications of GR, such as torsion theories of gravity. A class of theories allowing the presence of torsion is based on Riemann-Cartan spacetime, which is endowed with a metric $g_{\mu\nu}$ and a compatible connection. The resulting connection $\Gamma^{\lambda}_{\ \mu\nu}$ turns out to be nonsymmetric, and therefore it originates a non-vanishing torsion tensor. We refer to [5,6] for the details.

In standard torsion theories the source of torsion is considered to be the intrinsic spin of matter [5–8], which is negligible when averaged over a macroscopic body. Therefore spacetime torsion would be observationally negligible in the solar system. Nevertheless, in [9] Mao, Tegmark, Guth and Cabi (MTGC) argue that the presence of detectable torsion in the solar system should be tested experimentally, rather than derived by means of a specific torsion model. For this reason, in [9] a theory-independent framework based on symmetry arguments is developed, and it is determined by a set $t_1, t_2, w_1, \ldots, w_5$ of seven parameters describing torsion and three further parameters $\mathcal{F}, \mathcal{G}, \mathcal{H}$ describing the metric. Here, by theory-independent framework, we mean the following: the metric and the connection are parametrized, around a massive body, with the help of symmetry arguments, without reference to a torsion model based on a specific Lagrangian (or even on specific field equations).

This parametrized framework can be used to constrain $t_1, t_2, w_1, \ldots, w_5$ from solar system experiments. In particular, MTGC suggest that GPB [10] is an appropriate experiment for this task, and in [9] they compute precessions of gyroscopes and put constraints on torsion parameters from GPB measurements. In [11] Hehl and Obukhov argue that measuring torsion requires intrinsic spin, and criticize the approach of MTGC, since GPB gyroscopes do not carry uncompensated elementary particle spin. Nevertheless, we accept the general idea that the precise form of the coupling of torsion to matter should be tested experimentally, and that actual experimental knowledge leaves room for nonstandard torsion theories which could yield detectable torsion signals in the solar system. In the present paper we apply the parametrized framework developed by MTGC for the computation of satellites orbits around Earth and we put a different set of constraints on torsion parameters from SLR measurements.

MTGC also address the question of whether there exists a specific gravitational Lagrangian fitting in the parametrized framework and yielding a torsion signal

[1] International Laser Ranging Service; see http://www.ilrs.gsfc.nasa.gov/.

detectable by the GPB experiment. As an example they quote the theory of Hayashi and Shirafuji (HS) in [12] where a massive body generates a torsion field, and they propose what they call the Einstein-Hayashi-Shirafuji (EHS) Lagrangian, interpolating GR and HS Lagrangians in a linear way. However, MTGC consider only a gravitational Lagrangian in vacuum, so that they cannot derive the equations of motion of test bodies from the gravitational field equations, which would require a suitable matter coupling.

The EHS model has been criticized by various authors. In the paper [13], Flanagan and Rosenthal show that the linearized EHS theory becomes consistent only if the coefficients in the Lagrangian are constrained in such a way that the resulting predictions coincide with those of GR. In the paper [14], Puetzfeld and Obukhov derive the equations of motion in the framework of metric-affine gravity theories, which includes the HS theory, and show that only test bodies with microstructure (such as spin) can couple to torsion. In conclusion, the EHS theory does not yield a torsion signal detectable for GPB. For these reasons, in [9] the EHS Lagrangian is proposed not as a viable physical model, but as a pedagogical toy model fitting in the parametrized framework, and giving an illustration of the constraints that can be imposed on torsion by the GPB experiment. In the present paper we will not consider such a toy model.

As also remarked by Flanagan and Rosenthal in [13], the failure of constructing the specific EHS Lagrangian does not rule out the possibility that there may exist other torsion theories which could be usefully constrained by solar system experiments. Such torsion models should fit in the above mentioned theory-independent framework, similarly to a parametrized post-Newtonian framework including torsion. We remark that the parametrized formalism of MTGC does not take into account the intrinsic spin of matter as a possible source of torsion, and in this sense it cannot be a general torsion framework. However, it is adequate for the description of torsion around macroscopic massive bodies in the solar system, like planets, being the intrinsic spin negligible when averaged over such bodies.

Therefore we think it is worthwhile to continue the investigation of observable effects in the solar system of nonstandard torsion models within the MTGC parametrized formalism, under suitable working assumptions. In particular, our aim is to extend the GPB gyroscopes computations made in [9] to the case of motion of satellites.

In the present paper we compute the corrections to the orbital Lense-Thirring effect due to the presence of spacetime torsion described by $t_1, t_2, w_1, \ldots, w_5$. We consider the motion of a test body in the gravitational field of a rotating axisymmetric massive body, under the assumption of slow motion of the test body. Since we use a parametrized framework without specifying the coupling of torsion to matter, we cannot derive the equations of motion of test bodies from the gravitational field equations. Therefore, in order to compute effects of torsion on the orbits of satellites, we will work out the implications of the assumption that the trajectory of a test body is either an extremal or an autoparallel curve. Such trajectories do not need to coincide when torsion is present.

As in the original paper of Lense and Thirring [15], we characterize the motion using the six orbital elements of the osculating ellipse. In terms of these orbital elements, the equations of motion then reduce to the Lagrangian planetary equations.

We calculate the secular variations of the longitude Ω of the node and of the longitude $\widetilde{\omega}$ of the pericenter. The computed secular variations show how the corrections to the orbital Lense-Thirring effect depend on the torsion parameters, and it turns out that the dependence is only through $w_1, \ldots, w_5$. The data from the LAGEOS satellites are then used to constrain the relevant linear combinations of the torsion parameters. More precisely, we constrain two different linear combinations of $w_1, \ldots, w_5$ by using first the measurements of the nodes of LAGEOS and LAGEOS II, and then the measurements of the nodes of LAGEOS and LAGEOS II and of the perigee of LAGEOS II. In particular, torsion parameters cannot be constrained by satellite experiments in the case of extremal trajectories.

While the torsion perturbations to the Lense-Thirring effect depend only on $w_1, \ldots, w_5$, it turns out that another relevant relativistic effect, namely the geodetic precession (or de Sitter effect), depends on the parameters t_1 and t_2, and on a further parameter t_3. This latter parameter is involved in a higher order parametrization of torsion, which is necessary for the description of the geodetic precession effect, while it is not necessary at the order of accuracy required in the present paper. All computations of orbital geodetic precession with torsion of a satellite are performed in the companion paper [16], to which we will sometimes refer for details.

The paper is organized as follows. In Sect. 2 we briefly recall the notion of spacetime with torsion. In Sect. 3 we discuss the case of extremal trajectories. In Sect. 4 we analyze the equations of autoparallel trajectories and derive the related system of ordinary differential equations to first order. The expression of the system clearly reveals the perturbation due to torsion with respect to the Lense-Thirring equations. In Sect. 5 we derive the time evolution of the orbital elements, by applying the classical perturbation theory of Celestial Mechanics, in particular the Gauss form of the Lagrange planetary equations. In Sect. 6 we calculate the secular variations of the orbital elements. In Sect. 7 we recall some results from [16] where torsion solar perturbations are computed. These results will be used in Sect. 8, where we give the observational constraints that the LAGEOS experiment can place on torsion parameters. Conclusions are drawn in Sect. 9. For convenience of the reader, in the appendix (Sect. 10) we recall from [9] how to parametrize the metric and torsion tensors, and hence how to parametrize the connection, under suitable symmetry assumptions.

2 Spacetime with torsion

A manifold equipped with a Lorentzian metric $g_{\mu\nu}$ and a connection $\Gamma^{\lambda}{}_{\mu\nu}$ compatible with the metric is called a Riemann-Cartan spacetime [5,6]. Compatibility means that $\nabla_\mu g_{\nu\lambda} = 0$, where ∇ denotes the covariant derivative. We recall in particular that for any vector field v^λ

$$\nabla_\mu v^\lambda \equiv \partial_\mu v^\lambda + \Gamma^{\lambda}{}_{\mu\nu} v^\nu .$$

The connection is determined uniquely by $g_{\mu\nu}$ and by the torsion tensor

$$S_{\mu\nu}{}^{\lambda} \equiv \frac{1}{2}\left(\Gamma^{\lambda}{}_{\mu\nu} - \Gamma^{\lambda}{}_{\nu\mu}\right)$$

as follows:

$$\Gamma^{\lambda}_{\ \mu\nu} = \left\{ \begin{matrix} \lambda \\ \mu\nu \end{matrix} \right\} - K_{\mu\nu}^{\ \ \lambda}, \tag{2.1}$$

where $\{\cdot\}$ is the Levi-Civita connection, defined by

$$\left\{ \begin{matrix} \lambda \\ \mu\nu \end{matrix} \right\} = \frac{1}{2} g^{\lambda\rho} \left(\partial_\mu g_{\nu\rho} + \partial_\nu g_{\mu\rho} - \partial_\rho g_{\mu\nu} \right), \tag{2.2}$$

and

$$K_{\mu\nu}^{\ \ \lambda} \equiv -S_{\mu\nu}^{\ \ \lambda} - S^{\lambda}_{\ \nu\mu} - S^{\lambda}_{\ \mu\nu} \tag{2.3}$$

is the contortion tensor. In the particular case when $\Gamma^{\lambda}_{\ \mu\nu}$ is symmetric with respect to μ, ν the torsion tensor vanishes. We will be concerned here with the case of non-symmetric connections $\Gamma^{\lambda}_{\ \mu\nu}$. The case of vanishing torsion tensor corresponds to Riemann spacetime of GR, while the case of vanishing Riemann tensor corresponds to the Weitzenböck spacetime [12].

In the present paper we use the natural gravitational units $c = 1$ and $G = 1$. We will assume that Earth can be approximated as a uniformly rotating spherical object of mass m and angular momentum J. Following [9], we use spherical coordinates (r, θ, ϕ) for a satellite moving in the gravitational field of Earth, and we introduce the dimensionless parameters $\epsilon_m \equiv m/r$ and $\epsilon_J \equiv J/(mr)$. Since the radii of the LAGEOS orbits (about 6,000 km altitude) are much larger than Earth's Schwarzschild radius, it follows that $\epsilon_m << 1$. Moreover, since Earth is slowly rotating, we have $\epsilon_J << 1$. Therefore, all computations will be carried out perturbatively to first order in ϵ_m and ϵ_J.

Under spherical axisymmetry assumptions, the metric tensor $g_{\mu\nu}$ and the torsion tensor $S_{\mu\nu}^{\ \ \rho}$ have been parametrized to first order in [9]. Accordingly, $g_{\mu\nu}$ is parametrized by three parameters $\mathcal{H}, \mathcal{F}, \mathcal{G}$, and $S_{\mu\nu}^{\ \ \rho}$ is parametrized by seven parameters $t_1, t_2, w_1, \ldots, w_5$,

$$S_{\mu\nu}^{\ \ \lambda} = S_{\mu\nu}^{\ \ \lambda}\left(t_1, t_2, w_1, \ldots, w_5, r, \theta, \phi\right).$$

Therefore $\Gamma^{\lambda}_{\ \mu\nu}$ becomes an explicit function of all metric and torsion parameters. It turns out that t_1, t_2 contribute to geodetic precession, while $w_1, \ldots, w_5$ contribute to the frame-dragging precession. In the Appendix we report the explicit expressions of the parametrized metric and torsion tensors, and of the connection, that will be needed in the sequel of the paper.

3 Equations of extremal trajectories

In GR structureless test bodies move along geodesics. In a Riemann-Cartan spacetime there are two different classes of curves, autoparallel and extremal curves, respectively, which reduce to the geodesics of Riemann spacetime when torsion is zero [5].

Autoparallels are curves along which the velocity vector is transported parallel to itself by the connection $\Gamma^{\lambda}_{\mu\nu}$. Extremals are curves of extremal length with respect to the metric $g_{\mu\nu}$. The velocity vector is transported parallel to itself along extremal curves by the Levi-Civita connection. In GR the two types of trajectories coincide while, in general, they may differ in presence of torsion. They are identical when the torsion is totally antisymmetric [5], a condition which is not satisfied within our parametrization.

The equations of motion of bodies in the gravitational field follow from the field equations due to the Bianchi identities. The method of Papapetrou [17] can be used to derive the equations of motion of a test body with internal structure, such as for instance a small extended object that may have either rotational angular momentum or net spin. In standard torsion theories the trajectories of test bodies with internal structure, in general, are neither autoparallels nor extremals [5,6,18], while structureless test bodies, such as spinless test particles, follow extremal trajectories.

The precise form of the equations of motion of bodies in the gravitational field depends on the way the matter couples to the metric and the torsion in the Lagrangian (or in the gravitational field equations). As explained in the Introduction, we do not specify a coupling of torsion to matter, hence we do not specify the field equations. Moreover, in our computations of orbits of a satellite (considered as a test body), we will neglect its internal structure. In a theory-independent framework we cannot derive the equations of motion from the gravitational field equations, hence we need some working assumptions on the trajectories of structureless test bodies: we will investigate the consequences of the assumption that the trajectories are either extremal or autoparallel curves. Assuming the trajectory to be an extremal is natural and consistent with standard torsion theories. However, extremals depend only on the parameters of the metric, so that new predictions related to torsion cannot arise. We will quickly report the computations for the sake of completeness, since the metric parameters can be immediately related to the Parametrized Post Newtonian (PPN) parameters (see (10.2)), and the orbital Lense-Thirring effect in the case of extremal trajectories and a PPN metric is known.

The system of equations of extremal trajectories reads as

$$\frac{d^2x^{\lambda}}{d\tau^2} + \left\{ \begin{matrix} \lambda \\ \mu\nu \end{matrix} \right\} \frac{dx^{\mu}}{d\tau} \frac{dx^{\nu}}{d\tau} = 0, \tag{3.1}$$

where τ is the proper time. For slow motion of the satellite we can make the substitution $d\tau \simeq dt$, so that

$$\frac{d^2x^{\alpha}}{dt^2} + \left\{ \begin{matrix} \alpha \\ \mu\nu \end{matrix} \right\} \frac{dx^{\mu}}{dt} \frac{dx^{\nu}}{dt} = 0,$$

for $\alpha \in \{1, 2, 3\}$. We assume that the velocity of the satellite is small enough so that we can neglect the quadratic terms in the velocity. Then, being $x^0 = t$ we have

$$\frac{d^2x^{\alpha}}{dt^2} + \left\{ \begin{matrix} \alpha \\ 00 \end{matrix} \right\} + 2 \left\{ \begin{matrix} \alpha \\ 0\beta \end{matrix} \right\} \frac{dx^{\beta}}{dt} = 0, \tag{3.2}$$

for $\beta \in \{1, 2, 3\}$.

All perturbations considered here are so small that can be superposed linearly. Since we are only interested in the perturbations due to Earth's rotation, as in the original Lense-Thirring paper [15] we are allowed to neglect the quadratic terms in the velocities which yield an advance of the perigee of the satellite. The value of the advance of the perigee for an extremal orbit and a PPN metric can be found in [2, Chapter 7, formula (7.54)].

We use for x^α spherical coordinates (r, θ, ϕ). The Levi-Civita connection $\{\cdot\}$ can be obtained from the expression of $\Gamma^\lambda_{\mu\nu}$ given in the Appendix by setting to zero all torsion parameters $t_1, t_2, w_1, \ldots, w_5$. Substituting the resulting expression in (3.2) one gets

$$\begin{cases} \ddot{r}r - (\mathcal{H}/2)\epsilon_m + \mathcal{G}\dot{\phi}r\sin^2\theta\epsilon_m\epsilon_J = 0, \\ \ddot{\theta}r - 2\mathcal{G}\dot{\phi}\sin\theta\cos\theta\epsilon_m\epsilon_J = 0, \\ \ddot{\phi}r^2\sin\theta - \mathcal{G}\dot{r}\sin\theta\epsilon_m\epsilon_J + 2\mathcal{G}\dot{\theta}r\cos\theta\epsilon_m\epsilon_J = 0. \end{cases} \tag{3.3}$$

The equations of motions (3.3) depend neither on the metric parameter $\mathcal{F}$ nor on the torsion parameters. System (3.3) to lowest order becomes

$$\frac{d\vec{v}}{dt} = \frac{\mathcal{H}}{2}\frac{m}{r^2}\hat{e}_r,$$

where $\hat{e}_r$ is the unit vector in the radial direction. Imposing the Newtonian limit yields $\mathcal{H} = -2$ as in a PPN metric (see also [9, formula (23)]).

We now transform (3.3) in rectangular coordinates $x = r\sin\theta\cos\phi$, $y = r\sin\theta\sin\phi$, $z = r\cos\theta$. We compute the second derivatives of x, y, z with respect to time in the approximation of slow motion. Neglecting all terms containing squares and products of first derivatives with respect to (r, θ, ϕ), we get

$$\begin{cases} \ddot{x} = \ddot{r}\sin\theta\cos\phi + \ddot{\theta}r\cos\theta\cos\phi - \ddot{\phi}r\sin\theta\sin\phi, \\ \ddot{y} = \ddot{r}\sin\theta\sin\phi + \ddot{\theta}r\cos\theta\sin\phi + \ddot{\phi}r\sin\theta\cos\phi, \\ \ddot{z} = \ddot{r}\cos\theta - \ddot{\theta}r\sin\theta. \end{cases} \tag{3.4}$$

Using (3.3) and (3.4) we obtain the following system for the equations of motion:

$$\begin{cases} \ddot{x} = -\dfrac{\epsilon_m}{r^2}x - \mathcal{G}\dfrac{\epsilon_m\epsilon_J}{r^3}\left[\left(x^2 + y^2 - 2z^2\right)\dot{y} + 3yz\dot{z}\right], \\ \ddot{y} = -\dfrac{\epsilon_m}{r^2}y + \mathcal{G}\dfrac{\epsilon_m\epsilon_J}{r^3}\left[\left(x^2 + y^2 - 2z^2\right)\dot{x} + 3xz\dot{z}\right], \\ \ddot{z} = -\dfrac{\epsilon_m}{r^2}z + \mathcal{G}\dfrac{\epsilon_m\epsilon_J}{r^3}3z\left(y\dot{x} - x\dot{y}\right). \end{cases} \tag{3.5}$$

Note that when $\mathcal{G} = -2$ system (3.5) reduces to the equations of motion found by the Lense-Thirring [15, formula (15)]. Hence the relativistic perturbation of the Newtonian force is just multiplied by the factor $-\mathcal{G}/2$ with respect to the original Lense-Thirring equations. It follows that the formulae of precession of the orbital

elements of a satellite can be obtained by multiplying the original Lense-Thirring formulae [15, formula (17)] by the factor $-\mathcal{G}/2$. The details of the computation, based on the Lagrange planetary equations of Celestial Mechanics, can be also retrieved from the computations for autoparallel trajectories given in the next sections, by setting to zero all torsion parameters $t_1, t_2, w_1, \ldots, w_5$.

Using the standard astronomical notation, we denote by Ω the longitude of the node and by ω the argument of the perigee of the satellite's orbit. The secular contributions to the variations of Ω and ω are:

$$(\delta\Omega)_{\text{sec}} = -\frac{\mathcal{G}J}{a^3(1-e^2)^{3/2}}\,t, \quad (\delta\omega)_{\text{sec}} = \frac{3\mathcal{G}J\cos i}{a^3(1-e^2)^{3/2}}\,t, \tag{3.6}$$

where a is the semimajor axis of the satellite's orbit, e is the eccentricity, i is the orbital inclination, and t is time. When $\mathcal{G} = -2$ the quantities in (3.6) reduce to the classical corresponding Lense-Thirring ones.

Since the expressions of $(\delta\Omega)_{\text{sec}}$ and $(\delta\omega)_{\text{sec}}$ depend only on $\mathcal{G}$, the measurements of satellites experiments cannot be used to constrain the torsion parameters.

4 Equations of autoparallel trajectories

In standard torsion theories the trajectories of structureless test bodies follow extremal trajectories [5,6], which depend only on the metric. However, new predictions related to torsion may arise when considering the autoparallel trajectories. In the following we give some motivations which make worthwhile the investigation of autoparallel trajectories.

Since in spacetime with torsion parallelograms are in general not closed, but exhibit a closure failure proportional to the torsion, Kleinert and Pelster argue in [19] that the variational procedure in the action principle for the motion of structureless test bodies must be modified. In the standard variational procedure for finding the extrema of the action, paths are varied keeping the endpoints fixed in such a way that variations form closed paths. However, in the formalism of [19], the closure failure makes the variation at the final point nonzero, and this gives rise to a force due to torsion. When this argument is applied to the action principle for structureless test bodies it turns out that the resulting torsion force changes extremal trajectories to autoparallel ones (see [19] for the details). Kleinert and Shabanov find an analogous result in [20] where they show that the geometry of spacetime with torsion can be induced by embedding its curves in a euclidean space without torsion. Kleinert et al. also argue in [19,20] that autoparallel trajectories are consistent with the principle of inertia, since a structureless test body will change its direction in a minimal way at each time, so that the trajectory is as straight as possible.

The approach of Kleinert et al. has been criticized by Hehl and Obukhov in [11] since the equations of autoparallel trajectories have not been derived from the energy-momentum conservation laws. Kleinert investigates this issue in [21] and finds that, due to the closure failure, the energy-momentum tensor of spinless point particles

satisfies a different conservation law with respect to the one satisfied in torsion theories such as [5,6]. The resulting conservation law yields autoparallel trajectories for spinless test particles. Kleinert then addresses the question of whether this new conservation law allows for the construction of an extension of Einstein field equations to spacetime with torsion. The author gives an answer for the case of torsion derived from a scalar potential (see [6] for a discussion of this kind of torsion). In this case the autoparallel trajectories are derived from the gravitational field equations via the Bianchi identities, though the field equation for the scalar field, which is the potential of torsion, is unknown.

In [22] Dereli and Tucker show that the theory of Brans-Dicke can be reformulated as a field theory on a spacetime with dynamic torsion determined by the gradient of the Brans-Dicke scalar field. Then in [23] they suggest that the autoparallel trajectory of a spinless test particle in such a torsion geometry is a possibility that has to be taken into account. In [23] the autoparallel trajectories of massive spinless test particles are analyzed in the background of a spherically symmetric, static solution to the Brans-Dicke theory and the results are applied to the computations of the orbit of Mercury. In [24] the autoparallel trajectories of spinless particles are analyzed in the background of a Kerr Brans-Dicke geometry. In [25,26] the equations of autoparallel trajectories are derived from the gravitational field equations and Bianchi identities, in the special case of matter modeled as a pressureless fluid, and torsion expressed solely in terms of the gradient of the Brans-Dicke scalar field.

The above quoted results show that there is an interest in the autoparallels in spacetime with torsion, which make worthwhile their investigation in the present paper. The system of equations of autoparallels reads as

$$\frac{d^2x^\lambda}{d\tau^2} + \Gamma^\lambda_{\mu\nu}\frac{dx^\mu}{d\tau}\frac{dx^\nu}{d\tau} = 0, \tag{4.1}$$

where τ is the proper time [27]. Observe that only the symmetric part $\frac{1}{2}(\Gamma^\lambda_{\mu\nu} + \Gamma^\lambda_{\nu\mu})$ of the connection enters in (4.1); moreover, starting from (4.1) the totally antisymmetric part of $S_{\lambda\mu\nu}$ cannot be measured.

The trajectory of a test body has to be a time-like curve. Since the connection is compatible with the metric, the quantity $g_{\mu\nu}\frac{dx^\mu}{d\tau}\frac{dx^\nu}{d\tau}$ is conserved by parallel transport. The tangent vector $\frac{dx^\mu}{d\tau}$ to the trajectory undergoes parallel transport by the connection along the autoparallel. Therefore, an autoparallel that is time-like at one point has this same orientation everywhere, so that the trajectory is strictly contained in the light cone determined by $g_{\mu\nu}$, in a neighbourhood of every of its points. Hence the compatibility of the connection with the metric ensures that autoparallels fulfil a necessary requirement for causality.

For slow motion of the satellite we can make the substitution $d\tau \simeq dt$, so that

$$\frac{d^2x^\alpha}{dt^2} + \Gamma^\alpha_{\mu\nu}\frac{dx^\mu}{dt}\frac{dx^\nu}{dt} = 0,$$

for $\alpha \in \{1, 2, 3\}$. Again, we assume that the velocity of the satellite is small enough so that we can neglect the terms which are quadratic in the velocity. Then, being $x^0 = t$ we have

$$\frac{d^2x^\alpha}{dt^2} + \Gamma^\alpha_{00} + (\Gamma^\alpha_{\beta 0} + \Gamma^\alpha_{0\beta})\frac{dx^\beta}{dt} = 0, \tag{4.2}$$

for $\beta \in \{1, 2, 3\}$.

As in the previous section, all the perturbations that we are considering here are so small that can be superposed linearly. We are allowed to neglect the quadratic terms in the velocities which yield an advance of the perigee of the satellite. Such an advance of the perigee for an autoparallel orbit in presence of torsion has been computed in [16].

We use for x^α spherical coordinates (r, θ, ϕ). Substituting in (4.2) the expression of $\Gamma^\lambda_{\mu\nu}$ given in the Appendix one gets

$$\begin{cases} \ddot{r}r + \mathcal{C}\epsilon_m + \mathcal{D}\dot{\phi}r\sin^2\theta\epsilon_m\epsilon_J = 0, \\ \ddot{\theta}r - \mathcal{B}\dot{\phi}\sin\theta\cos\theta\epsilon_m\epsilon_J = 0, \\ \ddot{\phi}r^2\sin\theta + \mathcal{A}\dot{r}\sin\theta\epsilon_m\epsilon_J + \mathcal{B}\dot{\theta}r\cos\theta\epsilon_m\epsilon_J = 0, \end{cases} \tag{4.3}$$

where

$$\begin{cases} \mathcal{A} = -\mathcal{G} + w_1 - w_3, \\ \mathcal{B} = 2\mathcal{G} + w_2 - w_4, \\ \mathcal{C} = t_1 - \dfrac{\mathcal{H}}{2}, \\ \mathcal{D} = \mathcal{G} - w_1 - w_5. \end{cases} \tag{4.4}$$

Note that equations of motions (4.3) do not depend on the metric parameter $\mathcal{F}$ and on the torsion parameter t_2. Moreover, the dependence on w_2 and w_4 appears only through their difference.

System (4.3) to lowest order becomes

$$\frac{d\vec{v}}{dt} = -\mathcal{C}\frac{m}{r^2}\hat{e}_r,$$

where $\hat{e}_r$ is the unit vector in the radial direction. Imposing the Newtonian limit it follows that (see also [9, formula (23)])

$$\mathcal{C} = 1. \tag{4.5}$$

Since the Newtonian limit fixes the value of t_1, the equations of autoparallels depend only on the parameters $w_1, \ldots, w_5$ (called frame-dragging torsion parameters in [9]). Therefore the precession of satellite's orbital elements will depend only on such torsion parameters, as it has been found in [9] for gyroscopes.

Using (4.3) and (3.4) we obtain the following system for the equations of motion:

$$\begin{cases} \ddot{x} = -\dfrac{\epsilon_m}{r^2}x + \dfrac{\epsilon_m\epsilon_J}{r^3}\Big[(\mathcal{D}+\mathcal{A})xy\dot{x} + \left(-\mathcal{D}x^2 + \mathcal{A}y^2 + \mathcal{B}z^2\right)\dot{y} + (\mathcal{A}-\mathcal{B})\,yz\dot{z}\Big], \\ \ddot{y} = -\dfrac{\epsilon_m}{r^2}y + \dfrac{\epsilon_m\epsilon_J}{r^3}\Big[-(\mathcal{D}+\mathcal{A})xy\dot{y} + \left(-\mathcal{A}x^2 + \mathcal{D}y^2 - \mathcal{B}z^2\right)\dot{x} - (\mathcal{A}-\mathcal{B})\,xz\dot{z}\Big], \\ \ddot{z} = -\dfrac{\epsilon_m}{r^2}z + \dfrac{\epsilon_m\epsilon_J}{r^3}(\mathcal{D}+\mathcal{B})z\,(y\dot{x} - x\dot{y})\,. \end{cases} \tag{4.6}$$

Note that in case of no torsion (i.e. $w_i = 0$ for any $i = 1, \ldots, 5$) and when $\mathcal{G} = -2$ system (4.6) reduces to the equations of motion found by the Lense-Thirring [15, formula (15)].

5 Computation of orbital elements via perturbation theory

The system (4.6) expressing the motion along autoparallel trajectories can be written in the form

$$\begin{cases} \ddot{x} = -\dfrac{m}{r^3}x + F_x, \\ \ddot{y} = -\dfrac{m}{r^3}y + F_y, \\ \ddot{z} = -\dfrac{m}{r^3}z + F_z, \end{cases} \tag{5.1}$$

where (F_x, F_y, F_z) is the perturbation with respect to the Newton force,

$$\begin{cases} F_x = \dfrac{ma}{r^5}\Big[(\mathcal{D}+\mathcal{A})xy\dot{x} + \left(-\mathcal{D}x^2 + \mathcal{A}y^2 + \mathcal{B}z^2\right)\dot{y} + (\mathcal{A}-\mathcal{B})\,yz\dot{z}\Big], \\ F_y = \dfrac{ma}{r^5}\Big[-(\mathcal{D}+\mathcal{A})xy\dot{y} + \left(-\mathcal{A}x^2 + \mathcal{D}y^2 - \mathcal{B}z^2\right)\dot{x} - (\mathcal{A}-\mathcal{B})\,xz\dot{z}\Big], \\ F_z = \dfrac{ma}{r^5}(\mathcal{D}+\mathcal{B})z\,(y\dot{x} - x\dot{y})\,. \end{cases} \tag{5.2}$$

We use the standard coordinates transformation [28,29] used in Celestial Mechanics

$$\begin{cases} x = r\,(\cos u\cos\Omega - \sin u\sin\Omega\cos i)\,, \\ y = r\,(\cos u\sin\Omega + \sin u\cos\Omega\cos i)\,, \\ z = r\sin u\sin i, \end{cases}$$

where i is the orbital inclination, Ω is the longitude of the node, and u is the argument of latitude. The vector (F_x, F_y, F_z) can be decomposed in the standard way along three mutually orthogonal axes as

$$\begin{cases} S = \dfrac{x}{r}F_x + \dfrac{y}{r}F_y + \dfrac{z}{r}F_z, \\ T = \dfrac{\partial(x/r)}{\partial u}F_x + \dfrac{\partial(y/r)}{\partial u}F_y + \dfrac{\partial(z/r)}{\partial u}F_z, \\ \sin u\ W = \dfrac{\partial(x/r)}{\partial i}F_x + \dfrac{\partial(y/r)}{\partial i}F_y + \dfrac{\partial(z/r)}{\partial i}F_z. \end{cases} \tag{5.3}$$

Here S is the component along the instantaneous radius vector, T is the component perpendicular to the instantaneous radius vector in the direction of motion, and W is the component normal to the osculating plane of the orbit (colinear with the angular momentum vector). Then, substituting (5.2) into (5.3) gives

$$\begin{cases} S = -\dfrac{J}{r^2}\mathcal{D}\cos i\ \dot{u}, \\ T = -\dfrac{J}{r^3}\mathcal{A}\cos i\ \dot{r}, \\ W = \dfrac{J}{r^3}\sin i\ (\mathcal{A}\cos u\ \dot{r} - \mathcal{B}\sin ur\ \dot{u})\,. \end{cases} \tag{5.4}$$

Note that in case of no torsion and when $\mathcal{G} = -2$ formulae (5.4) reduce to the components found by Lense-Thirring (see equations (16) in [15]).

Let us now recall [28,29] that, using the method of variation of constants,

$$r = \frac{a(1-e^2)}{1+e\cos v},$$

where a is the semimajor axis of the satellite's orbit, e is the eccentricity, v is the true anomaly, and

$$\dot{r} = \frac{r^2 e\sin v}{a(1-e^2)}\dot{v}, \quad r^2\dot{v} = na^2(1-e^2)^{1/2},$$

$n = 2\pi/U$, U the period of revolution. Following the standard astronomical notation, we let ω be the argument of the perigee, and $\widetilde{\omega} = \Omega + \omega$ be the longitude of the perigee.

We also recall the following planetary equations of Lagrange in the Gauss form [29, Chapter 6, Sect. 6]:

$$\begin{cases} \dfrac{da}{dt} = \dfrac{2}{n(1-e^2)^{1/2}}\left[Se\sin v + T\,\dfrac{a(1-e^2)}{r}\right], \\ \dfrac{de}{dt} = \dfrac{(1-e^2)^{1/2}}{na}\left[S\sin v + T\left(e + \dfrac{r+a}{a}\cos v\right)\right], \\ \dfrac{di}{dt} = \dfrac{1}{na^2(1-e^2)^{1/2}}\,Wr\cos u, \\ \dfrac{d\Omega}{dt} = \dfrac{1}{na^2(1-e^2)^{1/2}\sin i}\,Wr\sin u, \\ \dfrac{d\widetilde{\omega}}{dt} = \dfrac{(1-e^2)^{1/2}}{nae}\left[-S\cos v + T\left(1 + \dfrac{r}{a(1-e^2)}\right)\sin v\right] + 2\sin^2\dfrac{i}{2}\,\dfrac{d\Omega}{dt}, \\ \dfrac{dL_0}{dt} = -\dfrac{2}{na^2}\,Sr + \dfrac{e^2}{1+(1-e^2)^{1/2}}\,\dfrac{d\widetilde{\omega}}{dt} + 2(1-e^2)^{1/2}\sin^2\dfrac{i}{2}\,\dfrac{d\Omega}{dt}, \end{cases} \tag{5.5}$$

where $L_0 = -\tau n + \widetilde{\omega}$ is the longitude at epoch, and τ is the time of periapsis passage.

Using the expressions of S, T and W given by (5.4) and integrating the Lagrange planetary equations we compute the variations of the orbital elements. According

to perturbation theory, we regard the orbital elements as approximately constant in the computation of such integrals. Since $u = v + \widetilde{\omega} - \Omega$, we can make use of the approximation

$$\dot{u} \simeq \dot{v}. \tag{5.6}$$

Inserting (5.4)–(5.6) into (5.5) yields

$$\begin{cases} \dfrac{da}{dt} = -\dfrac{2Je\cos i\ (1+e\cos v)^2\sin v}{na^2(1-e^2)^{5/2}}\left(\mathcal{A}\dot{v}+\mathcal{D}\dot{u}\right), \\ \dfrac{de}{dt} = -\dfrac{J\cos i\sin v}{na^3(1-e^2)^{3/2}}\Big[e(e+2\cos v+e\cos^2 v)\mathcal{A}\dot{v}+(1+e\cos v)^2\mathcal{D}\dot{u}\Big], \\ \dfrac{di}{dt} = \dfrac{J\sin i\cos u}{na^3(1-e^2)^{3/2}}\Big[e\sin v\cos u\mathcal{A}\dot{v}-\sin u(1+e\cos v)\mathcal{B}\dot{u}\Big], \\ \dfrac{d\Omega}{dt} = \dfrac{J\sin u}{na^3(1-e^2)^{3/2}}\Big[e\sin v\cos u\mathcal{A}\dot{v}-\sin u(1+e\cos v)\mathcal{B}\dot{u}\Big], \\ \dfrac{d\widetilde{\omega}}{dt} = \dfrac{J\cos i}{na^3e(1-e^2)^{3/2}}\Big[(1+e\cos v)^2\cos v\mathcal{D}\dot{u}-e\sin^2 v(2+e\cos v)\mathcal{A}\dot{v}\Big] \\ \qquad +2\sin^2\frac{i}{2}\frac{d\Omega}{dt}, \\ \dfrac{dL_0}{dt} = \dfrac{2J\cos i}{na^3(1-e^2)}(1+e\cos v)\mathcal{D}\dot{u}+\dfrac{e^2}{1+(1-e^2)^{1/2}}\dfrac{d\widetilde{\omega}}{dt} \\ \qquad +2(1-e^2)^{1/2}\sin^2\frac{i}{2}\frac{d\Omega}{dt}. \end{cases} \tag{5.7}$$

Recalling (5.6), we now integrate (5.7) with respect to v. Therefore we find for the variations of the orbital elements:

$$\delta a = \frac{2Je\cos i\cos v}{na^2(1-e^2)^{5/2}}\ (\mathcal{A}+\mathcal{D})\left(1+e\cos v+\frac{1}{3}e^2\cos^2 v\right),$$

$$\delta e = \frac{J\cos i\cos v}{na^3(1-e^2)^{3/2}}\left[(\mathcal{A}+\mathcal{D})\left(1+e\cos v+\frac{1}{3}e^2\cos^2 v\right)-\mathcal{A}(1-e^2)\right],$$

$$\delta i = \frac{J\sin i}{12na^3(1-e^2)^{3/2}}\Big[4(\mathcal{A}+2\mathcal{B})e\cos v\cos^2 u-4(\mathcal{B}+2\mathcal{A})e\cos v$$
$$+2(\mathcal{B}+2\mathcal{A})e\sin v\sin(2u)+3\mathcal{B}\cos(2u)\Big],$$

$$\delta\Omega = \frac{J}{6na^3(1-e^2)^{3/2}}\Big\{-3\mathcal{B}v+\frac{3\mathcal{B}}{2}\sin(2u)$$
$$+e\Big[2(\mathcal{A}-\mathcal{B})\sin v+(\mathcal{A}+2\mathcal{B})\sin(2u)\cos v-2(2\mathcal{A}+\mathcal{B})\sin v\cos^2 u\Big]\Big\},$$

$$\delta\widetilde{\omega} = \frac{J}{na^3e(1-e^2)^{3/2}}\cos i\ \Big\{\sin v\Big[\mathcal{D}+(\mathcal{A}+\mathcal{D})e\cos v+\frac{1}{3}(2\mathcal{D}-\mathcal{A})e^2$$
$$+\frac{1}{3}(\mathcal{A}+\mathcal{D})e^2\cos^2 v\Big]+(\mathcal{D}-\mathcal{A})ev\Big\}+2\sin^2\frac{i}{2}\,\delta\Omega,$$

$$\delta L_0 = \frac{2J\cos i}{na^3(1-e^2)}\mathcal{D}\,(v + e\sin v) + \frac{e^2}{1+(1-e^2)^{1/2}}\,\delta\widetilde{\omega} + 2(1-e^2)^{1/2}\sin^2\frac{i}{2}\,\delta\Omega.$$

We note that the contributions of the components S and T to the derivative $\frac{da}{dt}$ are proportional to $\mathcal{D}\dot{u}$ and $\mathcal{A}\dot{v}$, respectively, with the same proportionality constant. Using the approximation $\dot{u} \simeq \dot{v}$ it turns out that in the classical Lense-Thirring case, where the torsion parameters vanish and $-\mathcal{A} = \mathcal{D} = \mathcal{G}$, there is a cancellation of such contributions in such a way that δa vanishes. Conversely, in presence of torsion, if the eccentricity of the orbit is nonzero, the contributions of the radial and of the tangential component of the perturbative force differ, so that δa does not vanish, yielding a periodic perturbation of the semimajor axis of the satellite's orbit.

6 Torsion corrections to the Lense-Thirring effect

We observe that only periodic terms appear in δa, δe and δi. Secular terms appear in $\delta\Omega$, $\delta\widetilde{\omega}$ and δL_0. Since $v = nt +$ periodic terms in v, the secular contributions to the variations of the corresponding orbital elements are:

$$\begin{cases} (\delta\Omega)_{\rm sec} = -\dfrac{J}{2a^3(1-e^2)^{3/2}}\,\mathcal{B}t, \\ (\delta\widetilde{\omega})_{\rm sec} = \dfrac{J}{a^3(1-e^2)^{3/2}}\left[\mathcal{D}-\mathcal{A}-(\mathcal{B}+2\mathcal{D}-2\mathcal{A})\sin^2\dfrac{i}{2}\right]t, \\ (\delta L_0)_{\rm sec} = \dfrac{J}{a^3(1-e^2)}\left\{2\mathcal{D} + \dfrac{e^2}{1+(1-e^2)^{1/2}}\,\dfrac{1}{(1-e^2)^{1/2}}\right. \\ \qquad\qquad \left.\left[\mathcal{D}-\mathcal{A}-(\mathcal{B}+2\mathcal{D}-2\mathcal{A})\sin^2\tfrac{i}{2}\right] - (\mathcal{B}+4\mathcal{D})\sin^2\dfrac{i}{2}\right\}t. \end{cases} \tag{6.1}$$

In the absence of torsion and when $\mathcal{G} = -2$, it turns out that $(\delta\widetilde{\omega})_{\rm sec} = (\delta L_0)_{\rm sec}$, as found by Lense-Thirring.

Using (4.4) we rewrite (6.1). For the nodal rate we obtain

$$(\delta\Omega)_{\rm sec} = -\frac{\mathcal{G}J}{a^3(1-e^2)^{3/2}}\Big(1+\mu_1\Big)\,t, \tag{6.2}$$

and for the longitudinal rate of the perigee

$$(\delta\widetilde{\omega})_{\rm sec} = \frac{2\mathcal{G}J}{a^3(1-e^2)^{3/2}}\left[1+\mu_2-3\big(1+\mu_3\big)\sin^2\frac{i}{2}\right]t. \tag{6.3}$$

Since $\widetilde{\omega} = \Omega + \omega$, for the rate of the argument of the perigee we find

$$(\delta\omega)_{\rm sec} = \frac{\mathcal{G}J}{a^3(1-e^2)^{3/2}}\left[3+\mu_1+2\mu_2-6\,(1+\mu_3)\sin^2\frac{i}{2}\right]t. \tag{6.4}$$

The parameters

$$\mu_1 \equiv \frac{w_2 - w_4}{2\mathcal{G}},$$
$$\mu_2 \equiv \frac{2w_1 - w_3 + w_5}{-2\mathcal{G}},$$
$$\mu_3 \equiv \frac{4w_1 - w_2 - 2w_3 + w_4 + 2w_5}{-6\mathcal{G}},$$

measure deviations from GR. Indeed, when there is no torsion we have $w_i = 0$ for $i = 1, \ldots, 5$. When, in addition, $\mathcal{G} = -2$ the metric is the weak field approximation of a Kerr-like metric, and $\mu_1 = \mu_2 = \mu_3 = 0$ and we get the classical Lense-Thirring formulae [15]. We also give the expression for the rate of the longitude at epoch, namely

$$(\delta L_0)_{\rm sec} = -\frac{2\mathcal{G}J}{a^3(1-e^2)}\left\{ -\frac{e^2}{1+(1-e^2)^{1/2}}\frac{1}{(1-e^2)^{1/2}}\Big(1+\mu_2\Big) - \Big(1+\mu_4\Big) \right.$$
$$\left. + \left[\Big(1+\mu_1\Big) + \frac{3e^2}{1+(1-e^2)^{1/2}}\frac{1}{(1-e^2)^{1/2}}\Big(1+\mu_3\Big) + 2\Big(1+\mu_4\Big)\right]\sin^2\frac{i}{2}\right\} t, \tag{6.5}$$

where

$$\mu_4 \equiv \frac{w_1 + w_5}{-\mathcal{G}}.$$

Note that $\mu_1, \ldots, \mu_4$ do not depend on $t_1, t_2, \mathcal{F}, \mathcal{H}$.

7 Torsion corrections to the geodetic precession

The secular perturbations of the orbital elements computed in the previous sections are not the only torsion induced perturbations that are expected. Indeed, a further contribution due to solar perturbation is present, namely the geodetic precession in presence of torsion. The corresponding perturbations of the orbital elements have been computed in the companion paper [16] and they depend only on the torsion parameters t_i.

Since we are interested in putting constraints on the frame-dragging torsion parameters $w_1, \ldots, w_5$, there is a relevant difference between the case of GPB gyroscopes considered in [9] and the present problem of orbits of satellites. In [9] the average gyroscope precession rate is expressed as

$$\left\langle \frac{d\vec{S}_0}{dt} \right\rangle = \vec{\Omega}_{\rm eff} \times \vec{S}_0,$$

where $\vec{S}_0$ is the angular momentum of the spinning gyroscope measured by an observer comoving with its center of mass, and the vector $\vec{\Omega}_{\rm eff}$ of the angular precession rate

is a linear combination of $\vec{\omega}_O$ (the orbital angular velocity vector of the gyroscope) and $\vec{\omega}_E$ (the rotational angular velocity vector of the Earth around its axis). In $\vec{\Omega}_{\text{eff}}$ the coefficient of $\vec{\omega}_O$ is a linear combination of the parameters t_i, while the coefficient of $\vec{\omega}_E$ is a linear combination of the parameters w_i. Since the GPB satellite has a polar orbit the vectors $\vec{\omega}_O$ and $\vec{\omega}_E$ are orthogonal. The contribution to the average precession due to $\vec{\omega}_O$ is the geodetic precession of the gyroscope, while the contribution due to $\vec{\omega}_E$ is frame-dragging, both in the presence of torsion. Therefore, in the GPB experiment [10], when measuring the projections of the average precession rate of a gyroscope on the two corresponding orthogonal directions, it turns out that the linear combinations of the t_i and of the w_i torsion parameters can be constrained separately.

On the other hand, in the case of orbital motion of satellites, in the presence of torsion the geodetic precession and the Lense-Thirring effect are superimposed as it happens in GR, in such a way that the precessions of the orbital elements are simultaneously influenced by both effects. In [16] it has been found that the contribution of geodetic precession depends on a linear combination of the torsion parameters t_i, while the contribution of frame-dragging computed in the previous sections depends on a linear combination of the parameters w_i. It turns out that the precession of orbital elements (such as the node and the perigee) both depend on t_i and w_i, in such a way that without a knowledge of the dependence of such precessions on t_i, it is not possible to put constraints on the w_i. The knowledge of the dependence on t_i corresponds exactly to the knowledge of the geodetic precession of the orbital elements in presence of torsion.

In GR it is known that the geodetic precession is independent of the orbital elements of the satellites (and therefore it is the same both for LAGEOS and the Moon). This property is used in GR in order to compute an upper bound to the uncertainty in modeling the geodetic precession, and in order to show that the result is negligible with respect to the uncertainty in the measurement of the Lense-Thirring effect (see [4], Supplementary Discussion). Such a result is important in order to extract the Lense-Thirring effect from LAGEOS data, and it is achieved thanks to the precision of the measurement of geodetic precession by means of lunar laser ranging (LLR) data [30].

In Sect. 8 we will show that the uncertainty in modeling the geodetic precession can be neglected also in presence of spacetime torsion. In particular, the upper bounds on the torsion parameters t_i found in [16] and recalled in the subsequent formula (7.4) will be useful in order to obtain such a conclusion. This is important in order to extract the Lense-Thirring effect from LAGEOS data also in the presence of torsion, and that will allow us to constrain suitable linear combinations of the parameters w_i separately. Hence, in the following we briefly need to report the results obtained in [16].

The geodetic precession of orbital elements of the satellite in the gravitational field of the Earth and the Sun (both supposed to be nonrotating) is computed, in a Sun-centered reference system. It is shown that, to the required order of accuracy, the corresponding metric is described by a further parameter $\mathcal{I} = 2(\beta - \gamma)$, where β is the usual PPN parameter, and the parametrization of the torsion tensor involves a further parameter t_3 (see [16] for the details).

The secular contributions to the precessions of the node and of the perigee due to torsion found in [16] are the following:

$$(\delta\Omega^{\rm Sun})_{\rm sec} = \frac{1}{4}\frac{M\nu_0}{\rho}\left(C_1 - C_2\frac{\nu_0}{n}\cos i\right)\,t,$$
$$(\delta\widetilde{\omega}^{\rm Sun})_{\rm sec} = \frac{1}{4}\frac{M\nu_0}{\rho}\left\{C_1 + C_2\frac{\nu_0}{n}\left[4 - \cos i - 5\sin^2 i\,\sin^2(\widetilde{\omega} - \Omega)\right]\right\}\,t, \quad (7.1)$$

where

$$C_1 \equiv 1 - \frac{\mathcal{H}}{2} + 2\mathcal{F} + 3t_2, \quad C_2 \equiv 1 + \frac{\mathcal{H}}{2} + \frac{\mathcal{H}^2}{2} - \mathcal{F} - \mathcal{I} + t_2 + 2t_3. \quad (7.2)$$

Here M is the mass of the Sun, ν_0 is the revolution angular velocity of the Earth around the Sun, and ρ is the distance of the Earth from the Sun.

Differently from the Lense-Thirring effect, the precessions (7.1) depend on the torsion parameters t_2 and t_3, and are independent of t_4; the parameter t_1 is identified using the Newtonian limit (4.5).

We recall that t_3 and t_4 enter the parametrization of torsion at the higher order of accuracy required in the computation of precessions (7.1).

The perturbations (7.1) have to be superimposed to the ones computed in Sect. 6.

The first term on the right hand sides of the two formulas in (7.1) can be interpreted as the geodetic precession effect, when torsion is present [16]: accordingly we set

$$(\delta\Omega^{\rm geo})_{\rm sec} = (\delta\widetilde{\omega}^{\rm geo})_{\rm sec} = \frac{C_1}{4}\frac{M\nu_0}{\rho}t. \quad (7.3)$$

In the PPN formalism we have

$$C_1 = 2 + 4\gamma + 3t_2, \quad C_2 = t_2 + 2(1 - \beta + t_3).$$

Using LLR data and Mercury radar ranging data respectively, the following upper bounds are given in [16, Sect. 13]:

$$|t_2| < 0.0128, \quad |1 - \beta + t_3| < 0.0286. \quad (7.4)$$

Since for LAGEOS satellites $\frac{\nu_0}{n} \sim 4.2 \times 10^{-4}$, we have

$$(\delta\Omega^{\rm Sun})_{\rm sec} \simeq (\delta\Omega^{\rm geo})_{\rm sec}, \quad (\delta\widetilde{\omega}^{\rm Sun})_{\rm sec} \simeq (\delta\widetilde{\omega}^{\rm geo})_{\rm sec}.$$

Taking into account the expression of C_1, we have

$$(\delta\Omega^{\rm geo})_{\rm sec} = (\delta\widetilde{\omega}^{\rm geo})_{\rm sec} = \frac{M\nu_0}{2\rho}\left(1 + 2\gamma + \frac{3}{2}t_2\right)t. \quad (7.5)$$

This formula yields the rate of geodetic precession around an axis which is normal to the ecliptic plane. The projection of this precession rate on the axis of rotation of Earth is obtained by multiplying $(\delta\Omega^{\rm geo})_{\rm sec}$ by $\cos\epsilon$, where $\epsilon = 23.5$ degrees is the angle between the Earth's equatorial plane and the ecliptic plane [31]: this gives the values of the geodetic precession in a Earth-centered reference system.

8 Constraining torsion parameters with LAGEOS

In this section we describe how the LAGEOS data can be used to extract a limit on the torsion parameters. We will assume in the following that all metric parameters take the same form as in the PPN formalism, according to (10.2). Recent limits on various components of the torsion tensor, obtained in a different torsion model based on the fact that background torsion may violate effective local Lorentz invariance, have been obtained in [32]. See also [33], where constraints on possible new spin-coupled interactions using a torsion pendulum are described.

8.1 Constraints from nodes measurement

Here we discuss how frame dragging torsion parameters can be constrained by the measurement of a suitable linear combination of the nodal rates of the two LAGEOS satellites.

Equation (6.2) can be rewritten as

$$(\delta\Omega)_{\rm sec} = \frac{2J}{a^3(1-e^2)^{3/2}}\Big(-\frac{\mathcal{G}}{2} - \frac{w_2 - w_4}{4}\Big)\, t = (\delta\Omega)^{\rm GR}_{\rm sec}\, b_\Omega, \tag{8.1}$$

where we have defined, similarly to [9] and [16], a multiplicative torsion "bias" relative to the GR prediction as

$$b_\Omega = \frac{(\delta\Omega)_{\rm sec}}{(\delta\Omega)^{\rm GR}_{\rm sec}} = -\frac{\mathcal{G}}{2} - \frac{w_2 - w_4}{4} = \frac{1}{2}\Big(1 + \gamma + \frac{\alpha_1}{4}\Big) - \frac{w_2 - w_4}{4}, \tag{8.2}$$

$(\delta\Omega)^{\rm GR}_{\rm sec} = \frac{2J}{a^3(1-e^2)^{3/2}}t$ being the Lense-Thirring precession in GR. We recall that the values of such precessions are 31 and 31.5 mas/yr for LAGEOS and LAGEOS II, respectively, where mas/yr denotes milli-arcseconds per year.

Let us now consider the contribution of the geodetic precession to the nodal rate. We write the secular contribution to the nodal rate, in a Earth-centered reference system, in the form

$$(\delta\Omega^{\rm geo})_{\rm sec}\cos\epsilon = (\delta\Omega^{\rm geo})^{\rm GR}_{\rm sec}\cos\epsilon\ \ b^{\rm geo}_\Omega, \tag{8.3}$$

where $b^{\rm geo}_\Omega$ depends on t_2. Precisely, taking into account that $(\delta\Omega^{\rm geo})^{\rm GR}_{\rm sec} = \frac{3Mv_0}{2\rho}t$ and using (7.5), we have

$$b^{\rm geo}_\Omega = \frac{1}{3}(1+2\gamma) + \frac{t_2}{2}. \tag{8.4}$$

Moreover, the following numerical constraints are set on PPN parameters γ and α_1 by Cassini tracking [34] and LLR data [3], respectively:

$$\gamma - 1 = (2.1 \pm 2.3)\times 10^{-5}, \quad |\alpha_1| < 10^{-4}. \tag{8.5}$$

From (8.5) it follows that the term $\frac{1}{3}(1+2\gamma)$ differs from 1 by a few part in 10^{-5}. Therefore, using (7.4), (8.4) and (8.5) we get

$$\left|b_{\Omega}^{\mathrm{geo}}-1\right| \simeq \left|\frac{t_2}{2}\right| < 0.0064. \tag{8.6}$$

The measurement of the Lense-Thirring effect in [4,35] is based on the following linear combination of the total nodal rates of the two LAGEOS satellites:

$$\delta\Omega_{\mathrm{I}}^{\mathrm{tot}} + \kappa\,\delta\Omega_{\mathrm{II}}^{\mathrm{tot}}, \tag{8.7}$$

where the subscripts I and II denote LAGEOS and LAGEOS II, respectively. Here the total nodal rate $\delta\Omega^{\mathrm{tot}}$ of a LAGEOS satellite denotes the nodal rate due to all kinds of perturbations, both gravitational and nongravitational. The coefficient $\kappa = 0.545$ is chosen to make the linear combination (8.7) independent of any contribution of the Earth's quadrupole moment J_2, which describes the Earth's oblateness.

In [4] the residual (observed minus calculated) nodal rates $\Delta(\delta\Omega_{\mathrm{I}})$, $\Delta(\delta\Omega_{\mathrm{II}})$ of the LAGEOS satellites are obtained analyzing nearly eleven years of laser ranging data. The residuals are then combined according to the linear combination $\Delta(\delta\Omega_{\mathrm{I}}) + \kappa\,\Delta(\delta\Omega_{\mathrm{II}})$, analogue to (8.7). The Lense-Thirring effect is set equal to zero in the calculated nodal rates. The linear combination of the residuals, after removal of the main periodic signals, is fitted with a secular trend which corresponds to 99% of the theoretical Lense-Thirring prediction of GR (see [4,35] for the details):

$$(\delta\Omega_{\mathrm{I}})_{\mathrm{sec}}^{\mathrm{GR}} + \kappa\,(\delta\Omega_{\mathrm{II}})_{\mathrm{sec}}^{\mathrm{GR}} = 48.2\ \mathrm{mas/yr}.$$

The total uncertainty of the measurement is $\pm 5\%$ of the value predicted by GR [4,35,36]. This uncertainty is a total error budget that includes all estimated systematic errors due to gravitational and non-gravitational perturbations, and stochastic errors. Such a result is quoted as a $1-\sigma$ level estimate in [37,38], though an explicit indication of this fact is missing in [4]. Eventually, the authors allow for a total $\pm 10\%$ uncertainty to include underestimated and unmodelled error sources [4]. In the following we assume a value of $\pm 10\%$ for the uncertainty of the measurement.

Using the upper bound (8.6), the uncertainty in modeling geodetic precession in the presence of torsion is

$$\begin{aligned}\left|b_{\Omega}^{\mathrm{geo}}-1\right| &\left[\left(\delta\Omega_{\mathrm{I}}^{\mathrm{geo}}\right)_{\mathrm{sec}}^{\mathrm{GR}} + \kappa\left(\delta\Omega_{\mathrm{II}}^{\mathrm{geo}}\right)_{\mathrm{sec}}^{\mathrm{GR}}\right]\cos\epsilon \\ &\leq 0.0064\,\frac{27.2}{48.2} \times \left[(\delta\Omega_{\mathrm{I}})_{\mathrm{sec}}^{\mathrm{GR}} + \kappa\,(\delta\Omega_{\mathrm{II}})_{\mathrm{sec}}^{\mathrm{GR}}\right],\end{aligned} \tag{8.8}$$

where $\left[(\delta\Omega_{\mathrm{I}}^{\mathrm{geo}})_{\mathrm{sec}}^{\mathrm{GR}} + \kappa\,(\delta\Omega_{\mathrm{II}}^{\mathrm{geo}})_{\mathrm{sec}}^{\mathrm{GR}}\right]\cos\epsilon = 27.2\,\mathrm{mas/yr}$ is the contribution from geodetic precession predicted by GR for LAGEOS satellites. Compared to the $\pm 10\%$ uncertainty in the measurement of the Lense-Thirring effect, the uncertainty in modeling geodetic precession can be neglected (as in [4,35]) even in the presence of

spacetime torsion. This is a consequence of the torsion limits set with the Moon and Mercury in [16].

Then we can apply the results of [4,35] to our computations with torsion, and we obtain

$$\left|(\delta\Omega_{\rm I})_{\rm sec}+\kappa(\delta\Omega_{\rm II})_{\rm sec}-0.99\left[(\delta\Omega_{\rm I})^{\rm GR}_{\rm sec}+\kappa(\delta\Omega_{\rm II})^{\rm GR}_{\rm sec}\right]\right| < 0.10\left[(\delta\Omega_{\rm I})^{\rm GR}_{\rm sec}+\kappa(\delta\Omega_{\rm II})^{\rm GR}_{\rm sec}\right],$$

where $(\delta\Omega_{\rm I})_{\rm sec}$ and $(\delta\Omega_{\rm II})_{\rm sec}$ are given by (8.1). Since the torsion bias b_Ω does not depend on the orbital elements of the satellite, we have

$$\frac{(\delta\Omega_{\rm I})_{\rm sec}+\kappa(\delta\Omega_{\rm II})_{\rm sec}}{(\delta\Omega_{\rm I})^{\rm GR}_{\rm sec}+\kappa(\delta\Omega_{\rm II})^{\rm GR}_{\rm sec}}=b_\Omega.$$

Hence, using (8.2), we can constrain a linear combination of the frame-dragging torsion parameters w_2, w_4, setting the limit

$$|b_\Omega-0.99|=\left|\frac{1}{2}\left(\gamma-1+\frac{\alpha_1}{4}\right)-\frac{w_2-w_4}{4}+0.01\right|<0.10,$$

which is shown graphically in Fig. 1, together with the other constraints on γ and α_1 [3].

Taking into account the numerical constraints (8.5) the limit on torsion parameters from LAGEOS becomes

$$\left|-\frac{w_2-w_4}{2}+0.02\right|<0.20$$

which implies

$$-0.36<w_2-w_4<0.44. \tag{8.9}$$

The constraint (8.9) on the torsion parameters depends on the quantitative assessment of the uncertainty of the measurement of the Lense-Thirring effect. However, the value 5–10% of the uncertainty reported in [4] has been criticized by several authors. For example Iorio argues in [37] that the uncertainty might be 15–45%. The previous computations show that the upper bound on the quantity

$$\left|-\frac{w_2-w_4}{4}+0.01\right|$$

is given by the uncertainty of the measurement, so that one can find the constraint on the linear combination of the torsion parameters w_2, w_4 corresponding to a different value of the uncertainty. For instance, if the value of the uncertainty of the measurement is $\pm 50\%$, the constraint on torsion parameters becomes

$$-1.96<w_2-w_4<2.04.$$

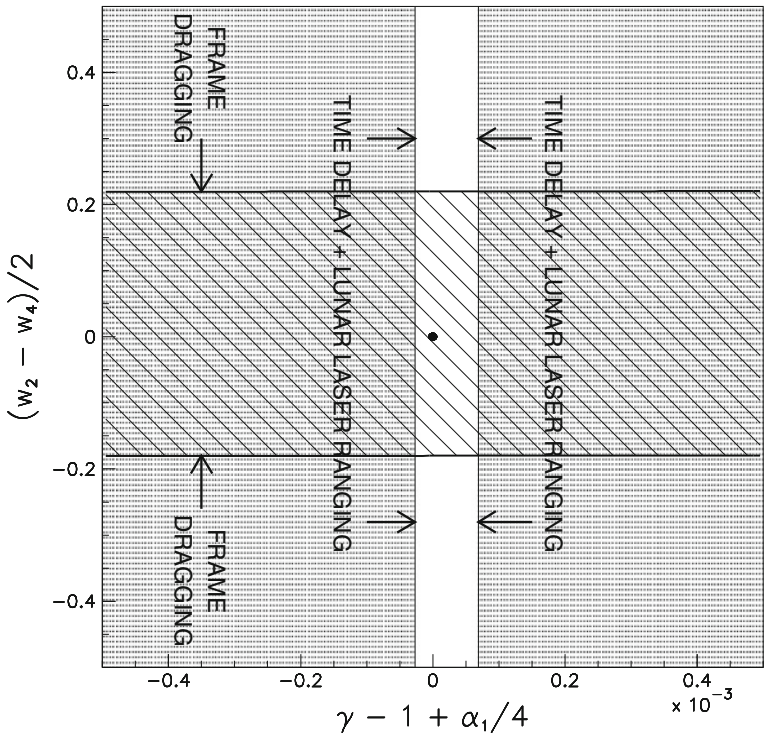

Fig. 1 constraints on PPN parameters (γ, α_1) and on frame-dragging torsion parameters (w_2, w_4) from solar system tests. The *grey area* is the region excluded by lunar laser ranging and Cassini tracking. The LAGEOS nodes measurement of the Lense-Thirring effect [4,35] excludes values of $(w_2 - w_4)/2$ outside the hatched region. General Relativity corresponds to $\gamma = 1, \alpha_1 = 0$ and all torsion parameters = 0 (*black dot*)

One of the goals of the LAGEOS, LAGEOS II, LARES[2] three-satellite experiment, together with improved Earth's gravity field models of GRACE (Gravity Recovery And Climate Experiment) is to improve the experimental accuracy on the orbital Lense-Thirring effect to "a few percent" [35].

We observe that, using (8.8) the uncertainty in modeling geodetic precession in presence of torsion amounts to about 0.4% of the Lense-Thirring effect, which is still a small contribution to a total root-square-sum error of a few percent. Note that an improved determination of the geodetic precession has been recently achieved by GPB [10] which, unlike LAGEOS, is designed to separate the frame-dragging and geodetic precessions by measuring two different, orthogonal precessions of its gyroscopes.

In the case of GPB, the torsion bias for the precession of a gyroscope is [9]

$$-\frac{\mathcal{G}}{2} - \frac{w_1 + w_2 - w_3 - 2w_4 + w_5}{2}.$$

[2] LAser RElativity Satellite, a geodynamics mission of the Italian Space Agency (ASI) to be launched.

This formula (the analogue of the right hand side of equation (8.2)) involves a linear combination of all frame-dragging torsion parameters. Such a linear combination can be constrained from GPB data. Since LAGEOS and GPB are sensitive to different linear combinations, together they can put more stringent torsion limits.

After taking into account the contribution of the geodetic precession, the combined constraints from gyroscope and orbital Lense-Thirring experiments are effective probes to search for the experimental signatures of spacetime torsion. In this sense, LAGEOS and GPB are to be considered complementary frame-dragging and, at the same time, torsion experiments, with the notable difference that GPB measures also the geodetic precession.

8.2 Constraints from nodes and perigee measurement

In this section we discuss how frame dragging torsion parameters can be constrained by the measurement of a linear combination of the nodal rates of LAGEOS and LAGEOS II and the perigee rate of LAGEOS II.

Similarly to the previous section, we define a multiplicative torsion "bias" relative to the GR prediction also for the rate of the argument of the perigee (6.4):

$$b_\omega = \frac{(\delta\omega)_{\rm sec}}{(\delta\omega)^{\rm GR}_{\rm sec}} = -\frac{\mathcal{G}}{6\cos i}\left[3+\mu_1+2\mu_2-6(1+\mu_3)\sin^2\frac{i}{2}\right],$$

$(\delta\omega)^{\rm GR}_{\rm sec} = -\frac{6J\cos i}{a^3(1-e^2)^{3/2}}t$ being the Lense-Thirring precession in GR: we recall that the value of this precession is -57mas/yr for LAGEOS II. In the following, the torsion bias b_ω is referred to LAGEOS II.

Using the values of μ_1, μ_2 and μ_3 given in Sect. 6 we find

$$b_\omega = -\frac{\mathcal{G}}{2} + \frac{4w_1 - w_2 - 2w_3 + w_4 + 2w_5}{12}. \tag{8.10}$$

The measurement of the Lense-Thirring effect in [39] is based on the following linear combination of the residuals of the nodes of LAGEOS and LAGEOS II and of the perigee of LAGEOS II:

$$\Delta(\delta\Omega_{\rm I}) + c_1\Delta(\delta\Omega_{\rm II}) + c_2\Delta(\delta\omega_{\rm II}), \tag{8.11}$$

where the coefficients $c_1 = 0.295$ and $c_2 = -0.35$ are chosen to make the linear combination (8.11) independent of the first two even zonal harmonic coefficients J_2 and J_4, and of their uncertainties.

In [39] the residuals are obtained analyzing 4 years of laser ranging data, and then combined according to the linear combination (8.11). The Lense-Thirring effect is set equal to zero in the calculated rates of the nodes and of the perigee. The linear combination of the residuals, after removal of the main periodic signals and of small observed inclination residuals, is fitted with a secular trend which corresponds to 1.1

times the theoretical Lense-Thirring prediction of GR (see [39] for the details):

$$(\delta\Omega_{\rm I})^{\rm GR}_{\rm sec} + c_1(\delta\Omega_{\rm II})^{\rm GR}_{\rm sec} + c_2(\delta\omega_{\rm II})^{\rm GR}_{\rm sec} = 60.2\ \text{mas/yr}.$$

The total uncertainty of the measurement found in [39] is $\pm 20\%$ of the value predicted by GR. This uncertainty is a total error budget that includes all the estimated systematic errors due to gravitational and non-gravitational perturbations. Such a result is quoted as a $1-\sigma$ level estimate in [37], though an explicit indication of this fact is missing in [39].

The contribution to the uncertainty of the measurement due to nongravitational perturbations, mainly thermal perturbative effects, on the perigee of LAGEOS II, amounts to 13% of the value predicted by GR. In [40] such an estimate is confirmed, however the author, when considering more pessimistic assumptions on some thermal effects, estimates that the contribution of nongravitational perturbations to the total uncertainty does not exceed the 28% of the GR value. Here we will follow this more conservative estimate. Inserting this value in the estimate of the total uncertainty computed in [39] yields a total root-square-sum error of 32% of the GR value.

For reasons similar to the ones discussed in the previous section, we are allowed to neglect the uncertainty in modeling the geodetic precession in presence of torsion. Then we can apply the results of [39] to our computations with torsion, and we obtain

$$\begin{aligned}&\left|(\delta\Omega_{\rm I})_{\rm sec} + c_1(\delta\Omega_{\rm II})_{\rm sec} + c_2(\delta\omega_{\rm II})_{\rm sec} - 1.1\left[(\delta\Omega_{\rm I})^{\rm GR}_{\rm sec} + c_1(\delta\Omega_{\rm II})^{\rm GR}_{\rm sec} + c_2(\delta\omega_{\rm II})^{\rm GR}_{\rm sec}\right]\right| \\ &< 0.32\left[(\delta\Omega_{\rm I})^{\rm GR}_{\rm sec} + c_1(\delta\Omega_{\rm II})^{\rm GR}_{\rm sec} + c_2(\delta\omega_{\rm II})^{\rm GR}_{\rm sec}\right].\end{aligned}$$

A direct computation gives

$$|(1-K)b_\Omega + Kb_\omega - 1.1| < 0.32, \tag{8.12}$$

where

$$K = \frac{c_2(\delta\omega_{\rm II})^{\rm GR}_{\rm sec}}{(\delta\Omega_{\rm I})^{\rm GR}_{\rm sec} + c_1(\delta\Omega_{\rm II})^{\rm GR}_{\rm sec} + c_2(\delta\omega_{\rm II})^{\rm GR}_{\rm sec}} = 0.33.$$

Inserting in (8.12) the expressions of b_Ω and b_ω given in (8.2), (8.10) and taking into account that $\mathcal{G} \simeq -2$ by formula (8.5), we obtain

$$-0.22 < -\frac{w_2 - w_4}{4} + K\left(\frac{2w_1 + w_2 - w_3 - w_4 + w_5}{6}\right) < 0.42.$$

Using the value of K we finally deduce

$$-0.22 < 0.11w_1 - 0.20w_2 - 0.06w_3 + 0.20w_4 + 0.06w_5 < 0.42, \tag{8.13}$$

which is shown graphically in Fig. 2, together with the other constraints on γ and α_1 [3]. The constraint (8.13) on the linear combination of the frame-dragging parameters

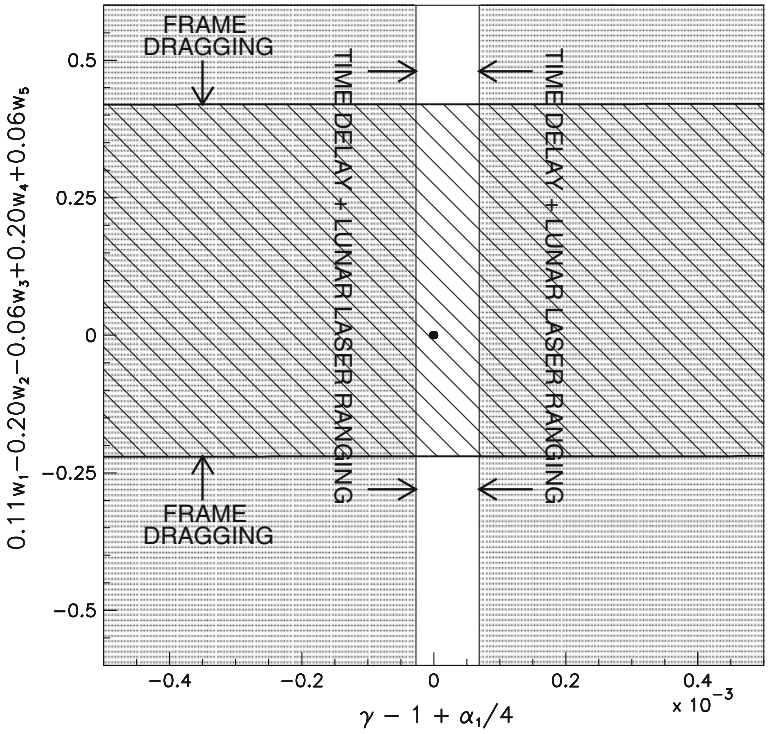

Fig. 2 constraints on PPN parameters (γ, α_1) and on frame-dragging torsion parameters $(w_1, w_2, w_3, w_4, w_5)$ from solar system tests. The *grey area* is the region excluded by lunar laser ranging and Cassini tracking. The LAGEOS nodes and perigee measurement of the Lense-Thirring effect [39,40] excludes values of $0.11w_1 - 0.20w_2 - 0.06w_3 + 0.20w_4 + 0.06w_5$ outside the hatched region. General Relativity corresponds to $\gamma = 1, \alpha_1 = 0$ and all torsion parameters = 0 (*black dot*)

is rather weak, due to the uncertainty on the nongravitational perturbations. Notice that the coefficients in front of w_3 and w_5 are of an order of magnitude smaller than the coefficients of the other parameters, so that the constraint on w_3 and w_5 is even looser.

Thermal thrusts (TTs) are the main source of non-gravitational perturbations [40]. One of the main drivers of LAGEOS TTs is the thermal relaxation time τ_{CCR} of its fused silica cube corner retroreflectors [41], which has been characterized in laboratory-simulated space conditions at the INFN-LNF Satellite/lunar laser ranging Characterization Facility (SCF) [42–44]. The measurements of LAGEOS τ_{CCR} in a variety of thermal conditions provide the basis for possibly reducing the uncertainty on the thermal perturbative effects. As a consequence, the constraint (8.13) could be improved.

The constraint (8.13) on the torsion parameters depends on the quantitative assessment of the uncertainty of the measurement of the Lense-Thirring effect. Again, the value ±20% of the uncertainty reported in [39] has been criticized by various authors. For example Ries, Eanes and Tapley argue in [45] that the uncertainty is at best in the 50–100% range. The uncertainty of the measurement yields the upper bound on the right-hand side of the estimate (8.12). Hence, one can find the constraint on the

linear combination of the torsion parameters w_i corresponding to a different value of the uncertainty as it has been discussed in Sect. 8.1.

We recall that in [9] an upper bound on the combination $|w_1 + w_2 - w_3 - 2w_4 + w_5|$ is given. This constrains the torsion parameters within two parallel hyperplanes in a five-dimensional space. If we couple this bound with our two estimates (8.9) and (8.13), we obtain that $w_1, \ldots, w_5$ are constrained to lye in a five-dimensional set, which is unbounded only along two directions. Hence, coupling GPB with SLR measurements significantly reduces the degrees of freedom on the frame-dragging parameters.

We conclude this section by observing that the recently approved JUNO mission to Jupiter [46] will make it possible, in principle, to attempt a measurement of the Lense-Thirring effect through the JUNO's node, which would be displaced by about 570 m over the mission duration of one year [47]. Hence, such a mission yields an opportunity for a possible improvement of the costraints on torsion parameters.

9 Conclusions

We have applied the framework recently developed in [9] for GR with torsion, to the computation of the slow orbital motion of a satellite in the field generated by the Earth. Starting from the autoparallel trajectories, we computed the corrections to the classical orbital Lense-Thirring effect in the presence of torsion. By using perturbation theory, we have found the explicit dependence of the secular variations of the longitudes of the node and of the perigee on the frame-dragging torsion parameters. The LAGEOS nodes measurements [4,35] and the LAGEOS nodes and perigee measurements [39,40] of the Lense-Thirring effect can be used to place constraints on torsion parameters, which are different and complementary to those set by GPB.

Acknowledgments We thank the University of Roma "Tor Vergata", CNR and INFN for supporting this work. We thank I. Ciufolini for suggesting this analysis after the publication of the paper by MTGC [9], and B. Bertotti and A. Riotto for useful advices.

10 Appendix

Under spherical axisymmetry assumptions, the metric tensor $g_{\mu\nu}$ can be parametrized to first order as follows [9]:

$$ds^2 = -\left[1 + \mathcal{H}\frac{m}{r}\right]dt^2 + \left[1 + \mathcal{F}\frac{m}{r}\right]dr^2 + r^2(d\theta^2 + \sin^2\theta\, d\phi^2) + 2\mathcal{G}\frac{J}{r}\sin^2\theta\, dt d\phi, \tag{10.1}$$

where $\mathcal{H}, \mathcal{F}, \mathcal{G}$ are three dimensionless parameters that can be immediately related to the Parametrized Post Newtonian (PPN) parameters:

$$\mathcal{H} = -2, \quad \mathcal{F} = 2\gamma, \quad \mathcal{G} = -\left(1 + \gamma + \frac{\alpha_1}{4}\right). \tag{10.2}$$

Here we follow the notation of the paper [9], instead of the PPN notation. This is useful in Sect. 7.

The nonvanishing components of the torsion tensor are:

$$
\begin{aligned}
S_{tr}{}^{t} &= t_1 \frac{m}{2r^2},\\
S_{r\theta}{}^{\theta} &= S_{r\phi}{}^{\phi} = t_2 \frac{m}{2r^2},\\
S_{r\phi}{}^{t} &= w_1 \frac{J}{2r^2} \sin^2\theta,\\
S_{\theta\phi}{}^{t} &= w_2 \frac{J}{2r} \sin\theta\cos\theta,\\
S_{t\phi}{}^{r} &= w_3 \frac{J}{2r^2} \sin^2\theta,\\
S_{t\phi}{}^{\theta} &= w_4 \frac{J}{2r^3} \sin\theta\cos\theta,\\
S_{tr}{}^{\phi} &= w_5 \frac{J}{2r^4},\\
S_{t\theta}{}^{\phi} &= -w_4 \frac{J}{2r^3} \frac{\cos\theta}{\sin\theta}.
\end{aligned}
\tag{10.3}
$$

The expression of the nonvanishing components of the connection approximated to first order in $\epsilon_m = m/r, \epsilon_J = J/(mr)$ and $\epsilon_m\epsilon_J = J/r^2$ is the following [9]:

$$
\begin{aligned}
\Gamma^{t}{}_{tr} &= \frac{1}{2r}\left(2t_1 - \mathcal{H}\right)\epsilon_m,\\
\Gamma^{t}{}_{rt} &= -\frac{\mathcal{H}}{2r}\,\epsilon_m,\\
\Gamma^{t}{}_{r\phi} &= \frac{1}{2}(3\mathcal{G} + (w_1 - w_3 - w_5))\sin^2\theta\,\epsilon_m\epsilon_J,\\
\Gamma^{t}{}_{\phi r} &= \frac{1}{2}(3\mathcal{G} - (w_1 + w_3 + w_5))\sin^2\theta\,\epsilon_m\epsilon_J,\\
\Gamma^{t}{}_{\theta\phi} &= \frac{1}{2}w_2 r\sin\theta\cos\theta\,\epsilon_m\epsilon_J,\\
\Gamma^{r}{}_{tt} &= \frac{1}{2r}\left(2t_1 - \mathcal{H}\right)\epsilon_m,\\
\Gamma^{r}{}_{rr} &= -\frac{\mathcal{F}}{2r}\,\epsilon_m,\\
\Gamma^{r}{}_{\theta\theta} &= -r + (t_2 + \mathcal{F})r\,\epsilon_m,\\
\Gamma^{r}{}_{\phi\phi} &= -r\sin^2\theta + \frac{1}{r}(\mathcal{F} + t_2)\sin^2\theta\,\epsilon_m,\\
\Gamma^{r}{}_{t\phi} &= \frac{1}{2}(\mathcal{G} - (w_1 - w_3 + w_5))\sin^2\theta\,\epsilon_m\epsilon_J,\\
\Gamma^{r}{}_{\phi t} &= \frac{1}{2}(\mathcal{G} - (w_1 + w_3 + w_5))\sin^2\theta\,\epsilon_m\epsilon_J,
\end{aligned}
$$

$$
\begin{aligned}
\Gamma^{\theta}_{t\phi} &= -\frac{1}{2r}(2\mathcal{G} + (w_2 - 2w_4))\sin\theta\cos\theta\,\epsilon_m\epsilon_J,\\
\Gamma^{\theta}_{\phi t} &= -\frac{1}{2r}(2\mathcal{G} + w_2)\sin\theta\cos\theta\,\epsilon_m\epsilon_J,\\
\Gamma^{\theta}_{r\theta} &= \Gamma^{\phi}_{r\phi} = \frac{1}{r},\\
\Gamma^{\theta}_{\theta r} &= \Gamma^{\phi}_{\phi r} = \frac{1}{r} - \frac{1}{r}t_2\,\epsilon_m,\\
\Gamma^{\theta}_{\phi\phi} &= -\sin\theta\cos\theta,\\
\Gamma^{\phi}_{tr} &= -\frac{1}{2r^2}(\mathcal{G} - (w_1 - w_3 + w_5))\,\epsilon_m\epsilon_J,\\
\Gamma^{\phi}_{rt} &= -\frac{1}{2r^2}(\mathcal{G} - (w_1 - w_3 - w_5))\,\epsilon_m\epsilon_J,\\
\Gamma^{\phi}_{t\theta} &= \frac{1}{2r}(2\mathcal{G} + (w_2 - 2w_4))\frac{\cos\theta}{\sin\theta}\,\epsilon_m\epsilon_J,\\
\Gamma^{\phi}_{\theta t} &= \frac{1}{2r}(2\mathcal{G} + w_2)\frac{\cos\theta}{\sin\theta}\,\epsilon_m\epsilon_J,\\
\Gamma^{\phi}_{\theta\phi} &= \Gamma^{\phi}_{\phi\theta} = \frac{\cos\theta}{\sin\theta}.
\end{aligned}
$$

References

1. Ciufolini, I., Wheeler, J.A.: Gravitation and Inertia. Princeton University Press, Princeton (1995)
2. Will, C.M.: Theory and Experiment in Gravitational Physics. Cambridge University Press, Cambridge (1993)
3. Will, C.M.: Living Rev. Relativ. **9**, 3 (2006) (www.livingreviews.org/lrr-2006-3)
4. Ciufolini, I., Pavlis, E.C.: Nature **431**, 958 (2004)
5. Hehl, F.W., von der Heyde, P., Kerlick, G.D., Nester, J.M.: Rev. Mod. Phys. **48**, 393 (1976)
6. Hammond, R.T.: Rep. Prog. Phys. **65**, 599 (2002)
7. Stoeger, W.R., Yasskin, P.B.: Gen. Relativ. Gravit. **11**, 427 (1979)
8. Yasskin, P.B., Stoeger, W.R.: Phys. Rev. D **21**, 2081 (1980)
9. Mao, Y., Tegmark, M., Guth, A.H., Cabi, S.: Phys. Rev. D **76**, 1550 (2007)
10. Everitt, C.W.F., et al.: Phys. Rev. Lett. **106**, 221101 (2011)
11. Hehl, F.W., Obukhov, Y.N.: Ann. Fondation Louis de Broglie **32**, 157 (2007)
12. Hayashi, K., Shirafuji, T.: Phys. Rev. D **19**, 3524 (1979)
13. Flanagan, E.F., Rosenthal, E.: Phys. Rev. D **75**, 124016 (2007)
14. Puetzfeld, D., Obukhov, Y.N.: Phys. Lett. A **372**, 6711 (2008)
15. Lense, J., Thirring, H.: Phys. Z. **19**, 156 (1918), translated in: B. Mashhoon, F.W. Hehl, D.S. Theiss, Gen. Relativ. Gravit. **16**(8), (1984)
16. March, R., Bellettini, G., Tauraso, R., Dell'Agnello, S.: Phys. Rev. D **83**, 104008 (2011)
17. Papapetrou, A.: Proc. R. Soc. A **209**, 248 (1951)
18. Babourova, O.V., Frolov, B.N.: Phys. Rev. D **82**, 27503 (2010)
19. Kleinert, H., Pelster, A.: Gen. Relativ. Gravit. **31**, 1439 (1999)
20. Kleinert, H., Shabanov, S.V.: Phys. Lett. B **428**, 315 (1998)
21. Kleinert, H.: Gen. Relativ. Gravit. **32**, 769 (2000)
22. Dereli, T., Tucker, R.W.: Phys. Lett. B **110**, 206 (1982)
23. Dereli, T., Tucker, R.W.: Mod. Phys. Lett. A **17**, 421 (2002)
24. Cebeci, H., Dereli, T., Tucker, R.W.: Int. J. Mod. Phys. D **13**, 137 (2004)
25. Dereli, T., Tucker, R.W.: arXiv gr-qc/0107017
26. Burton, D.A., Dereli, T., Tucker, R.W.: In: Aldaya, V., Cerveró, J.M., Garcia, Y.P. (eds) Symmetries in Gravity and Field Theory. Ediciones Universidad Salamanca, p. 237, 2004

27. Ponomariev, V.N.: Bull. Acad. Pol. Sci. **XIX**, 6 (1971)
28. Brouwer, D., Clemence, G.M.: Methods of Celestial Mechanics. Academic Press, New York (1961)
29. Geyling, F.T., Westerman, H.R.: Introduction to Orbital Mechanics. Addison Wesley, Reading (1971)
30. Williams, J.G., Turyshev, S.G., Boggs, D.H.: Phys. Rev. Lett. **93**, 261101 (2004)
31. Huang, C., Ries, J.C., Tapley, B.D., Watkins, M.M.: Celest. Mech. Dyn. Astron. **48**, 167 (1990)
32. Kostelecky, V.A., Russell, N., Tasson, J.: Phys. Rev. Lett. **100**, 111102 (2008)
33. Heckel, B.R., et al.: Phys. Rev. D **78**, 092006 (2008)
34. Bertotti, B., Iess, L., Tortora, P.: Nature **425**, 374 (2003)
35. Ciufolini, I., et al.: Space Sci. Rev. **148**, 71 (2009)
36. Ciufolini, I., Pavlis, E.C., Peron, R.: New Astron. **11**, 527 (2006)
37. Iorio, L.: New Astron. **10**, 603 (2005)
38. Lucchesi, D.M.: Adv. Space Res. **39**, 1559 (2007)
39. Ciufolini, I., et al.: Science **279**, 2100 (1998)
40. Lucchesi, D.M.: Plan. Space Sci. **50**, 1067 (2002)
41. Bosco, A., Cantone, C., Dell'Agnello, S., Delle Monache, G.O., et al.: Int. J. Mod. Phys. D **16**(12a), 2271 (2007)
42. Dell'Agnello, S., et al.: In: Proceedings of the 16th International Workshop on Laser Ranging, October 13–17, Poznan, Poland, 121, 2008
43. Dell'Agnello, S., et al.: Adv. Space Res., Galileo Special Issue **47**, 822–842 (2011)
44. Dell'Agnello, S., et al.: Exp. Astron., *MAGIA Special Issue*, doi:10.1007/s10686-010-9195-0 (2010)
45. Ries, J.C., Eanes, R.J., Tapley, B.D.: In: Ruffini, R., Sigismondi, C. (eds) Nonlinear Gravitodynamics. World Scientific, Singapore, p. 201, 2003
46. Matousek, S.: Acta Astronaut. **61**, 932 (2007)
47. Iorio, L.: New Astron. **15**, 554 (2010)